

# Engineering Notes

ENGINEERING NOTES are short manuscripts describing new developments or important results of a preliminary nature. These Notes cannot exceed 6 manuscript pages and 3 figures; a page of text may be substituted for a figure and vice versa. After informal review by the editors, they may be published within a few months of the date of receipt. Style requirements are the same as for regular contributions (see inside back cover).

## Experimental Stress Analysis of Propeller Blades Utilizing Photoelastic Coating Techniques

Hideya Tsushima\* and Joseph C. Conway†

The Pennsylvania State University,  
University Park, Pa.

### Introduction

IN designing and optimizing propeller blades of complex configuration, an analytical or numerical approach results in extremely complex equations which must usually be solved with the aid of a computer. Experimental stress analysis techniques, however, offer a direct and often more simplified approach.

The photoelastic coating technique gives the magnitude and direction of principal stresses as well as the location and intensity of probable stress concentrations on the surface of a component subjected to load.<sup>1</sup> It is particularly useful in qualitatively evaluating components of complex shape and in rapidly evaluating design modifications to prevent failure.

In this investigation, the technique was applied to a statically loaded, skewed propeller blade to demonstrate its feasibility. The blade was coated with a moldable photoelastic plastic and data was obtained with a commercial reflectance polariscope. Principal stress distributions were

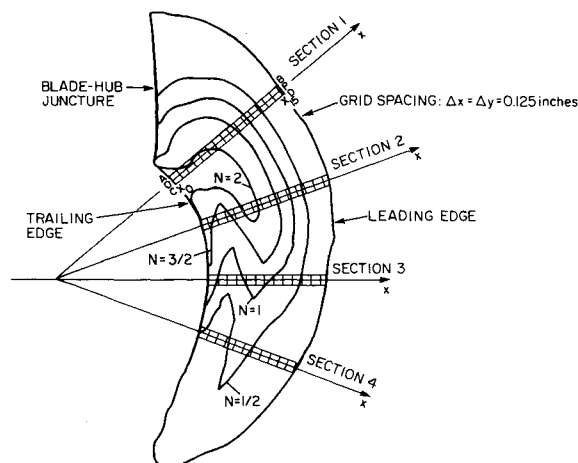


Fig. 2 Isochromatic fringe orders and shear difference grid locations for experimental propeller blade.

determined from photoelastic data at selected sections and are graphically portrayed.

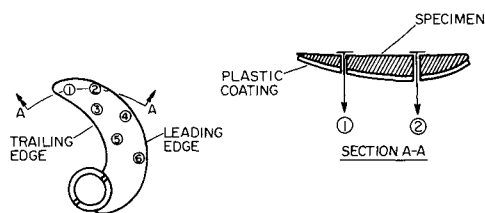
### Formulation of the Problem

The investigation was performed on an epoxy resin blade similar to an aluminum propeller designated as NSRDC 4143.<sup>2</sup> Use of the plastic blade resulted in easily measurable strains for the given loading condition. Measurement of mechanical properties indicated a modulus of elasticity of  $1.426 \times 10^6$  psi and Poisson's ratio of 0.36. Static loading, simulating the measured hydrostatic profile, was represented by six concentrated forces applied to selected points on the blade surface as shown in Fig. 1. The loading direction was parallel to the steady thrust force direction of the propeller, or parallel to the hub axis.

### Photoelastic Analysis

The experimental propeller blade was coated with moldable photoelastic plastic PL-1 supplied by Photoelastic Inc. The photoelastic coating had a stress fringe coefficient  $f$  of 66.3 psi/in./order, a modulus of elasticity of 420,000 psi and a Poisson's ratio of 0.36. The coating thickness averaged 0.096 in. The coating was molded to the surface in a state of partial polymerization and allowed to cure. It was then firmly bonded with the appropriate epoxy resin. After bonding, the coating was checked for the presence of residual stresses.

The photoelastic analysis consisted of 1) photographically recording isochromatic fringes or loci of maximum principle stress difference, 2) photographically recording isoclinics or loci of constant principle stress direction, 3) separating the principle stresses at selected sections on the blade surface through the use of shear difference techniques, and 4) adjusting the principle stresses to reflect the reinforcing effect of the birefringent coating. Integer- and half-order isochromatic fringes obtained for the loading condition shown in Fig. 1 can be seen in Fig. 2. Also shown in the same figure are shear difference grids along



|   | LOADING | LOCATION                |   |
|---|---------|-------------------------|---|
|   |         | RADIAL DISTANCE $x/r_0$ | CHORDWISE DISTANCE FROM LEADING EDGE, $y/c$ |
| ① | 5 lbs   | 0.9                     | 0.75  |
| ② | 5       | 0.9                     | 0.25  |
| ③ | 10      | 0.7                     | 0.75  |
| ④ | 10      | 0.7                     | 0.25  |
| ⑤ | 5       | 0.5                     | 0.75  |
| ⑥ | 5       | 0.5                     | 0.25  |

NOTE:  
1. LOADING DIRECTION IS PARALLEL TO THE HUB AXIS  
2.  $r_0$ , BLADE RADIUS  
3.  $c$ , LOCAL CHORD LENGTH

Fig. 1 Loading condition for experimental propeller blade.

Received May 22, 1972; revision received September 14, 1972. This research was supported by the Ordnance Research Laboratory, The Pennsylvania State University, under contract with the Naval Ordnance Systems Command.

Index category: Marine Vessel Design.

\* Graduate Assistant, Department of Aerospace Engineering.

† Assistant Professor, Department of Engineering Mechanics.

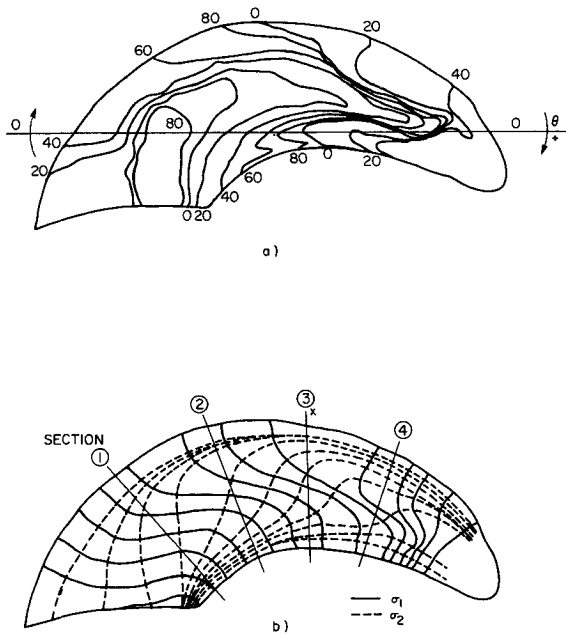


Fig. 3 a) Isoclinics and b) stress trajectories for experimental propeller blade.

selected sections of interest. Corresponding isoclinic data and resultant stress trajectories can be seen in Fig. 3.

Shear differencing was conducted along the four selected sections shown in Fig. 2. Shear stress distributions were generated along AB and CD for each section using the equation

$$\tau_{xy}^c \Big|_{x_n} = \frac{Nf\sigma}{4h} \sin 2\theta \quad (1)$$

where  $x_n$  is the distance to the  $n$ th grid point in the direction of integration (in.),  $\tau_{xy}^c$  is the shear stress in the coating (psi),  $N$  is the isochromatic fringe order,  $f\sigma$  is the stress fringe coefficient for the material (psi/in./order),  $h$  is the coating thickness (in.),  $\sigma$  is the angle from the X-axis to the maximum principal stress (degrees). The difference in shear  $\Delta\tau_{xy}^c = (\tau_{xy}^{cAB} - \tau_{xy}^{cCD})$  was then computed along each section and placed in the shear difference equation

$$\sigma_x^c \Big|_{x_{n+1}} = \sigma_x^c \Big|_{x_n} - \Delta\tau_{xy}^c \Big|_{\frac{x_n + x_{n+1}}{2}} \quad (2)$$

where  $\sigma_x^c$  is the normal coating stress in the direction of integration (psi), and  $\Delta\tau_{xy}^c$  is the shear difference in the coating (psi) to obtain the normal coating stress in the direction of integration. The normal stress perpendicular to the direction of integration was obtained from

$$\sigma_y^c \Big|_{x_n} = \sigma_x^c \Big|_{x_n} - \frac{Nf\sigma}{2h} \cos 2\theta \quad (3)$$

Finally, principal stresses in the coating were obtained from

$$\begin{aligned} \sigma_1^c &= 1/2 (\sigma_x^c + \sigma_y^c + Nf\sigma/2h) \\ \sigma_2^c &= 1/2 (\sigma_x^c + \sigma_y^c - Nf\sigma/2h) \end{aligned} \quad (4)$$

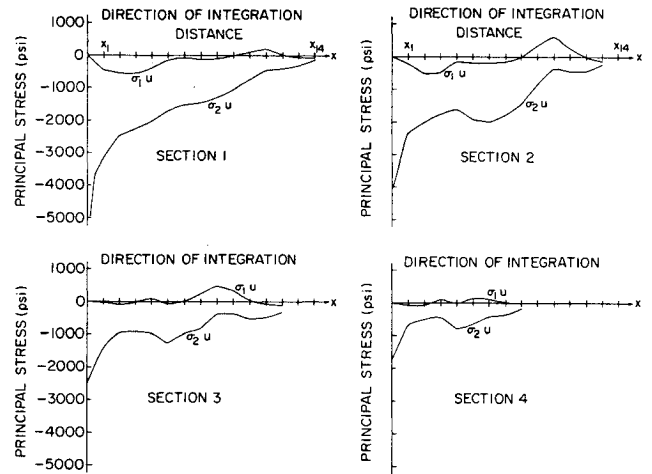


Fig. 4 Principal stress distributions at four selected sections of the uncoated experimental blade.

The principal stresses in the coating material were then converted to principal stresses in an uncoated specimen by using a correction factor

$$F_{CB} = \frac{1 + BC}{1 + C} \quad 4(1 + BC)^3 - \frac{3(1 - BC^2)^2}{1 + BC} \quad (5)$$

where

$$B = (E^c/E^s)[1 - \nu^{s^2}/(1 - \nu^{c^2})] \quad C = h^c/h^s$$

$E^c$  is the modulus of elasticity of coating (psi),  $E^s$  is the modulus of elasticity of the specimen (psi),  $\nu^c$  is the Poisson's ratio of the coating,  $\nu^s$  is the Poisson's ratio of the specimen,  $h^c$  is the thickness of the coating (in.),  $h^s$  is the thickness of the specimen (in.).

The correction factor considers the difference in geometry and mechanical properties of the coating and specimen as well as the reinforcing effect of the coating.<sup>3</sup> The principal stresses in the uncoated specimen were given as

$$\sigma_1^u = (F_{CB}/B) \sigma_1^c \quad \sigma_2^u = (F_{CB}/B) \sigma_2^c \quad (6)$$

where  $\sigma_1^u$  is the maximum principal stress in the uncoated blade (psi), and  $\sigma_2^u$  is the minimum principal stress in the uncoated blade (psi). Plots of maximum and minimum principal stress along the four selected sections of the uncoated blade can be seen in Fig. 4. Results, in general, compare well to those obtained in a separate study utilizing electrical resistance strain gages.<sup>4</sup>

## Conclusions

From experimental results, the following conclusions are established: 1) The photoelastic coating technique offers a simple and direct experimental means for analyzing and designing propeller blades of complex configuration. 2) For the propeller blade studied, high levels of principal stress are found along the trailing edge of the blade with the maximum level occurring at the blade-hub juncture. 3) Principal stress magnitude decreases from the blade root to the blade tip.

## References

- 1 Dally, W. J. and Riley, F. W., *Experimental Stress Analysis*, McGraw-Hill, New York, 1965, pp. 280-307.

<sup>2</sup> Denny, S. B., "Cavitation and Open-Water Performance Tests of a Series of Propellers Designed by Lifting-Surface Method," Rept. 2878, Sept. 1968, Dept. of the Navy, Naval Ship Research and Development Center, Washington, D.C., pp. 39-43.

<sup>3</sup> Timoshenko, S. and Woinowsky-Krieger, S., *Theory of Plates and Shells*, McGraw-Hill, New York, 1959, pp. 33-42.

<sup>4</sup> Boswell, R. J., "Static Stress Measurements on a Highly Skewed Propeller Blade," Rept. 3247, Dec. 1969, Dept. of the Navy, Naval Ship Research and Development Center, Washington, D.C., p. 6-7.

## Simplified Tradeoff Studies of Large Hydrofoil Ships

J. R. Greco\*

Naval Ship Engineering Center, Hyattsville, Md.

### Nomenclature

|                  |   |
|------------------|---|
| DHP              | = drag horsepower, hp   |
| $E_H$            | = endurance, hr   |
| $L/D$            | = dynamic lift/drag ratio   |
| $m_{TO}$         | = takeoff horsepower margin (percent of maximum intermittent horsepower possible)                                       |
| $P_L$            | = payload = 0.1 $W$ , tons  |
| $PR$             | = propeller type propulsor system   |
| $R$              | = range, naut miles   |
| SHP              | = maximum intermittent shaft horsepower (engine output), hp   |
| SFC              | = specific fuel consumption, lb/shp-hr  |
| $V$              | = speed, knots  |
| $V_{avg}$        | = average speed in sprint/drift mode, knots   |
| $V_{burst}$      | = burst speed, short duration capability, knots   |
| $V_{max}$        | = maximum continuous operational speed (at maximum continuous shaft hp, which is 85% of SHP), knots                     |
| $V_{min}$        | = minimum foilborne speed, knots  |
| $V_{TO}$         | = takeoff speed from hullborne to foilborne (Fig. 1), knots   |
| $W$              | = platform full-load displacement, tons   |
| $W_F$            | = fuel capacity, tons   |
| $W/S$            | = foil loading, psf   |
| $WJ$             | = waterjet type propulsor system  |
| $\eta$           | = propulsive coefficient, Fig. 1; product of transmission (from turbine output shaft) and propulsor system efficiencies |
| $\tau_D, \tau_S$ | = fractions of time drifting and sprinting, Eqs. (4-6)  |

### Subscripts

D, S = drift and sprint speed modes, respectively

### Introduction

THIS Note presents a simple analytical approach for examining first-order effects of major parameters on preliminary designs of large hydrofoil ships. Two design criteria are employed, which reflect the extremes of design speed emphasis: 1) design for a 25% margin ( $m_{TO}$ ) in horsepower at the takeoff speed  $V_{TO}$ , and 2) design for a maximum-burst-speed capability of 50 knots. The powerplants considered are marine gas turbines in three sizes which permit maximum intermittent shaft horsepower (SHP's) of 30,000, 40,000, and 50,000 hp. (Maximum con-

tinuous ratings, which determine maximum cruise speed  $V_{max}$ , are 85% of these SHP values.) The two foil loadings considered ( $W/S = 800$  and 1200 psf) are representative of current practical design bounds. The two propulsion types considered (propeller and waterjet) represent the limits (upper and lower respectively) of attainable propulsive efficiency  $\eta$ . This matrix of 2 criteria  $\times$  3 SHP's  $\times$  2 ( $W/S$ )s  $\times$  2 propulsor types produces 24 configurations.

### Configuration Designs

For each case, the desired design criterion and SHP,  $W/S$ , and propulsor type are specified. For the specified  $W/S$  and propulsor type, the associated ratio of drag-horsepower to full-load displacement ( $DHP/W$ ) and  $\eta$  are determined for the design speed of interest ( $V_{TO}$  or 50 knots, depending on the design criterion) from Fig. 1. Here  $DHP/W$  inversely reflects the  $L/D$  capability of the platform, and  $\eta$  is assumed to represent the over-all efficiency of the transmission (from turbine output shaft) and propulsor system. Then  $W$  is obtained from the desired design criterion. For the 25%  $m_{TO}$  criterion,  $m_{TO} = 0.25$   $DHP/W$ , and

$$W = \frac{\eta \cdot SHP}{1.25 (DHP/W)} \quad \Bigg| \quad V_{design} = V_{TO} \quad (1a)$$

For the 50-knot-burst-speed criterion,  $m_{V_{burst}} = 0$ , and

$$W = \frac{\eta \cdot SHP}{DHP/W} \quad \Bigg| \quad V_{design} = V_{burst} = 50 \text{ knots} \quad (1b)$$

Having determined  $W$ , and assuming 0.1 payload fraction ( $P_L/W = 0.1$ ), the fuel fraction is obtained from the  $(P_L + W_F)/W$  vs  $W$  curve (Fig. 2).

The 24 configurations derived are presented in Table 1. The 50-knot criterion yields lower displacements, except for the 1200/ $WJ$  cases. For the 1200-psf foil loading, the difference in the denominators in Eqs. (1a) and (1b) is smaller than the difference in waterjet efficiencies ( $\eta$ ) for the two design speeds ( $V_{TO} = 29$  knots;  $V_{burst} = 50$  knots). Similar reasoning associates maximum displacement with the 800/ $PR$  designs for the 25% margin criterion and with the 1200/ $PR$  designs for the burst-speed criterion.

The maximum burst speeds for the 25%  $m_{TO}$  criterion designs were graphically derived by plotting the speed-power curves developed from the powerplant shafthorsepowers and propulsive coefficients (available power) and the platform full load displacements and  $DHP/W$  ratio (required power). By plotting these power relationships as a function of speed, the intersection of the available power curve with the required power curve determines the maximum speed (burst) possible, which varies from 39 to 56 knots for the candidate platforms, with little difference between the 800/ $WJ$  and 1200/ $PR$  designs. The takeoff margins for the burst-speed-criterion designs are well over 25% except for the 1200/ $WJ$  designs, which have no margins.

### Platform Performance

For each of the 24 configurations, endurance  $E_H$  and range  $R$  can be calculated for various constant speeds

Received July 6, 1972; presented as Paper 72-595 at the AIAA/USNA/USN Advanced Marine Vehicles Meeting, Annapolis, Md., July 17-19, 1972; revision received October 10, 1972.

Index category: Surface Vessel Systems.

\*Operations Research Analyst.